Asymmetric design of photonic crystal surface-emitting lasers with low-threshold characteristics

Chih-Tsang Hung, Tsung-Lin Ho, and Tien-Chang Lu*

Department of Photonics and Institute of Electro-Optical Engineering, National Chiao Tung University, Hsinchu 30050, Taiwan

*Corresponding author: timtclu@mail.nctu.edu.tw

Received 29 April 2013; revised 7 July 2013; accepted 12 July 2013; posted 23 July 2013 (Doc. ID 189722); published 9 August 2013

We present AlGaAs-InGaAs multiquantum wells photonic crystal surface-emitting lasers by using the transfer matrix method and coupled wave method to achieve a low-threshold operation. The extremely low-threshold gain is achieved by adopting an asymmetric cladding layer design to enhance both of the vertical optical confinement factors for the quantum wells and photonic crystal (PC). By modifying the composition of the AlGaAs layer to raise the refractive index in the p-type cladding, optical field distribution will obviously be shifted to the p side. Hence, it results in a significant coupling enhancement between the optical mode profile and the PC layer. The optimized value of the vertically optical confinement factor of the PC layer is 13.94%, and the corresponding threshold gain can be as low as 19.45 cm^{-1}. © 2013 Optical Society of America

OCIS codes: (050.5298) Photonic crystals; (140.2020) Diode lasers.
http://dx.doi.org/10.1364/AO.52.005851

1. Introduction

In recent years, there have been more and more optoelectronics devices investigated and developed with photonic crystal (PC) structures. Two-dimensional (2D) PC surface-emitting lasers (PCSELs) have especially attracted much attention because of several outstanding properties, such as the single-mode output, ultrasmall divergence beam, and high-power operation [1–4]. The PC region strongly coupled with the optical field distribution in the vertical direction, and hence the systems, operate as surface-emitting lasers. By rigorously adjusting the normalized frequency at the photonic band edges and the PC period of the PCSELs, the specific Bragg diffraction will occur to achieve the surface emission condition [5–7]. Moreover, it can be achieved to manipulate both the beam profiles and their polarization by using a suitable structure of the PC unit cell and lattice phase [2,8]. On the other hand, GaAs-based semiconductor materials have generally been applied in several semiconductor lasers featured with visible and infrared lasers from many decades ago. Since the compound semiconductor manufacturing technologies are constantly moving forward, there are as many applications developed in media storage, optical pumping sources, industry processes, medical treatments, and various new facilities.

Regarding the conventional square-lattice PC structure with transverse electric (TE) polarization, surface emission is obtained around the Γ point, and the lasing oscillation happens at the mode possessing the lowest threshold gain at the edges of the band structure. To estimate the threshold gain of resonant modes at the band edges is quite important for these PCSELs to approach excellent device characteristics. An analysis on the variations of the threshold gains under the different oscillation modes might be rather hard when applying commonly used theoretical

1559-128X/13/235851-05$15.00/0
© 2013 Optical Society of America

means, such as the plane-wave expansion (PWE) method [9], the finite-difference time-domain method [10], and the time-domain Fourier–Galerkin method [11]. Nevertheless, the analysis on the mode threshold for finite-structure PC lasers can be simplified by calculating it with the coupled-wave model [12]. On the other hand, the calculation should be closer to the real situation as the vertical optical confinement factor is considered. We recently have demonstrated the influence of the vertically optical confinement factor on the optoelectronics characteristics of PCSEL devices by using the transfer matrix method (TMM) [9] and the relationship between the threshold gain and the filling factor of the square-lattice PC patterns by using the coupled-wave theory (CWT) [13] and PWE. In detail, we optimized the thickness of the cladding, optical confinement layers, and filling factor in the PCSEL structure [14]. Not only the air-hole type but also the dielectric-rod-type PC structures can be applied to the calculation procedure. In this article, we propose and design an asymmetric vertical structure by modifying the composition of p/n-type cladding layers in order to achieve a laser operation with an extremely low-threshold gain. The relationship between the filling factor and threshold gain has also been considered simultaneously.

2. Experimental Design

The multilayer laser structure of an AlGaAs-InGaAs PCSEL is shown in Fig. 1. We adopt a GaAs substrate with high n-type doping, and the layer sequence consists of an n-type 1.3 μm thick $Al_{0.3}Ga_{0.7}As$ bottom cladding layer, an AlGaAs-InGaAs active layer, a 100 nm thick PC layer followed by a 1.3 μm thick p-type top cladding layer with varied $Al_xGa_{(1-x)}As$ composition, and a 50 nm thick GaAs layer for ohmic contact formation. The active region includes a three-pair $In_{0.2}Ga_{0.8}As$/GaAs (6 nm/6.5 nm) multiple quantum well (MQW) surrounded within the 50 nm thick n-type and 130 nm thick p-type $Al_{0.15}Ga_{0.85}As$ optical confinement layers. To shift the distribution of the optical field close to the PC layer, we use an asymmetric cladding structure by adjusting the "x" factor of the p-type $Al_xGa_{(1-x)}As$ cladding layer. The PC layer

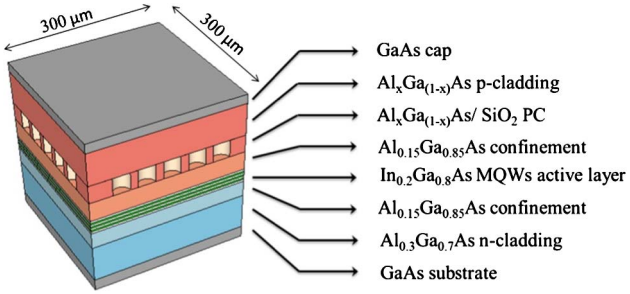

Fig. 1. The full structure of an AlGaAs-InGaAs PCSEL, which contains a GaAs substrate, an n-type AlGaAs bottom cladding layer, InGaAs-GaAs MQWs surrounded by two AlGaAs optical confinement layers, a PC layer followed by a p-type AlGaAs top cladding layer, and a p-type GaAs cap layer.

is composed of SiO_2 rods and a p-type AlGaAs base. The filling factor, which means "radius divided by period," is chosen as 0.15 in the 2D PC structure. The dimension of the PC area is set to be 300 μm × 300 μm defined as the cavity length.

We can use the CWT and TMM to acquire the distribution of the optical mode profile and the effective refractive index (n_{eff}) of the fundamental mode in the structures. Then, we can estimate the ratio of the optical field distribution within the PC region to figure out the optical confinement factor in the vertical direction. Hence, the effective index can be computed by the following approximated formulas [9]: $n_{\text{eff}}^2 = \text{ff} \times \varepsilon_a + (1 - \text{ff}) \times \varepsilon_b$ and $\Delta\varepsilon = \Gamma_{\text{PC}} \times (\varepsilon_{\text{bulk}} - \varepsilon_{\text{rod}})$, where ff is the filling factor, Γ_{PC} is the vertically optical confinement factor of the PC layer, $\Delta\varepsilon = \varepsilon_b - \varepsilon_a$, and $(\varepsilon_{\text{bulk}} - \varepsilon_{\text{rod}})$ is the difference between the two materials composing the PC layer. This procedure is an effective method to obtain the dielectric constants for the circular rod (ε_a) and the basis (ε_b) within the PC region that are applied to the calculation of the CWT to solve for the threshold gain [9].

We adopt a coupled-wave analysis for square-lattice PC lasers with TE polarization. Based on the eight-wave model, it is able to describe the coupling of two light waves propagating in the orthogonal direction. We derive the coupled-wave equations and coupling constants for the square lattice of the circular holes as shown in the following:

$$(\alpha - k_0 - i\delta)R_x - \frac{\partial}{\partial x}R_x = i\frac{4k_1^2}{\beta_0}R_x + (ik_3 - k_0)S_x + i\frac{2k_1^2}{\beta_0}S_y + i\frac{2k_1^2}{\beta_0}R_y,$$

$$(\alpha - k_0 - i\delta)S_x + \frac{\partial}{\partial x}S_x = i\frac{4k_1^2}{\beta_0}S_x + (ik_3 - k_0)R_x + i\frac{2k_1^2}{\beta_0}S_y + i\frac{2k_1^2}{\beta_0}R_y,$$

$$(\alpha - k_0 - i\delta)R_y - \frac{\partial}{\partial y}R_y = i\frac{4k_1^2}{\beta_0}R_y + (ik_3 - k_0)S_y + i\frac{2k_1^2}{\beta_0}S_x + i\frac{2k_1^2}{\beta_0}R_x,$$

$$(\alpha - k_0 - i\delta)S_y + \frac{\partial}{\partial y}S_y = i\frac{4k_1^2}{\beta_0}S_y + (ik_3 - k_0)R_y + i\frac{2k_1^2}{\beta_0}S_x + i\frac{2k_1^2}{\beta_0}R_x.$$

Here, α is the averaged gain constant $\beta_0 = 2\pi/a$, a is the lattice constant, k_0 is the vertical coupling constant related to the coupling constant k_1, and L is the length of PC cavity length. δ is a normalized frequency defined by $\delta \equiv (\beta^2 - \beta_0^2)/2\beta_0 \approx \beta - \beta_0 = n(\omega - \omega_0)/c$. R_x, S_x, R_y, and S_y are the complex amplitudes of the waves propagating along the x and y (Γ–X) direction. Coupling constant k_1 describes the intensity of the coupling of two plane waves

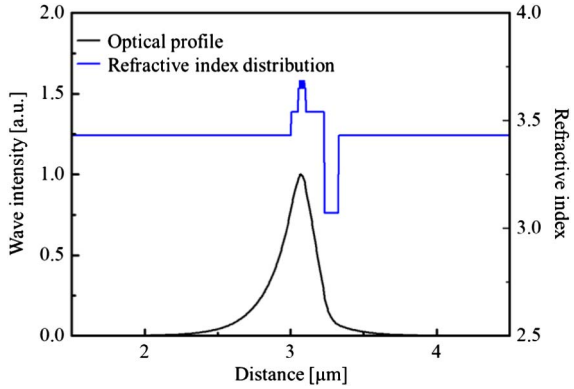

Fig. 2. Optical profile of the device in the vertical direction. The black and blue lines represent the optical field distribution and the refractive index in the structure, respectively.

propagating at 45° to each other, and k_3 describes the intensity of the coupling of the counterpropagating wave. The PC cavity length is $L = 300$ μm and the lattice constant is $a = 300$ nm. By numerically solving these equations under the boundary conditions, the eigenvalue α and δ provide the threshold gain (αL) and the frequency (δL) deviation from the Bragg condition, respectively.

The relation between optical field distribution and the refractive index of the PCSEL structure adopting a symmetric cladding design in the vertical direction (or along the growth direction) is shown in Fig. 2. The fundamental mode profile exhibits a skew Gaussian-like distribution and tends to shift close to the n-type cladding layer due to the insertion of the PC layer whose refractive index is much lower than the other layers around the active region into the structure of the surface-emitting laser. It leads to significant deterioration of the optical confinement coupled with MQWs and PC layers. The alteration of the effective index does not only come from the addition of SiO_2 rods, which possess an extremely low refractive index of 1.5, but it is also contributed from the variation of the filling factor. Figure 3 shows that the confinement factors vary as a function of the filling factor. Both the confinement factors of the PC and QW layers become weak constantly while the filling factor increases gradually from 0 to 1. In this investigation, we want to enhance the optical coupling effect on the MQWs and PC layers by modifying the Al content of the p-type AlGaAs cladding under a suitable filling factor. Whiles reducing the Al ratio to increase the refractive index of the p cladding, it attributes the optical mode profile to move toward the p-type region. Hence, the enhancement of the optical coupling effect on the MQWs and PC layers shall be obtained.

Concerning the optimizing procedures, we first choose the filling factor as 0.08, which is referenced from our previous investigation, and modify the Al content of the p-cladding layer to find better results of the vertically optical-confinement factor coupled with MQWs. Here, we fixed the Al content of the n-cladding layers and other parameters including the confinement layer. Finally, we used a 2D threshold gain mapping as functions of the PC filling factor and Al content of p cladding to obtain an optimized structure design of the PC structure, which can determine the effective refractive index to calculate the lowest threshold gain in our PCSELs.

3. Results and Discussion

As shown in Fig. 4, we can observe the relationship between the threshold gain and confinement factors with various AlGaAs compositions in the p cladding. The field profile will prefer to distribute away from the n-type cladding if we decrease the Al content to increase the refractive index of the p-side AlGaAs layer. It is helpful to raise the confinement factors of the QWs and PC layers. Comparing with the confinement factors of the MQWs, those of the PC layers are enhanced remarkably as the Al content is increased from 0.8 to 0.26. The main reason is that the PC layer possesses a lower refractive index; thus, it cannot couple with the fundamental mode profile efficiently until the optical field is shifted sufficiently close to the p-type region. However, both of the confinement factors deteriorate rapidly when the Al ratio is

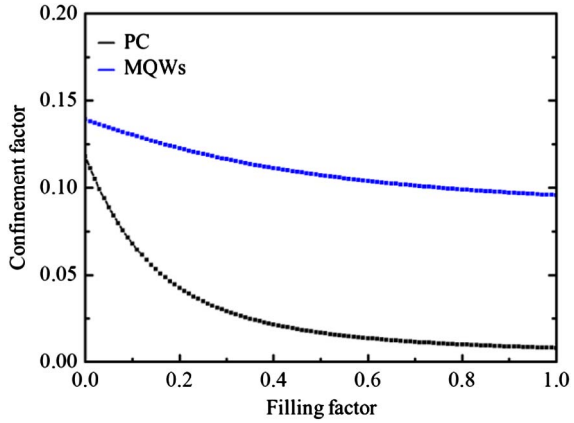

Fig. 3. Confinement factors of the PC layer and quantum wells decrease with increasing the filling factor of the PC.

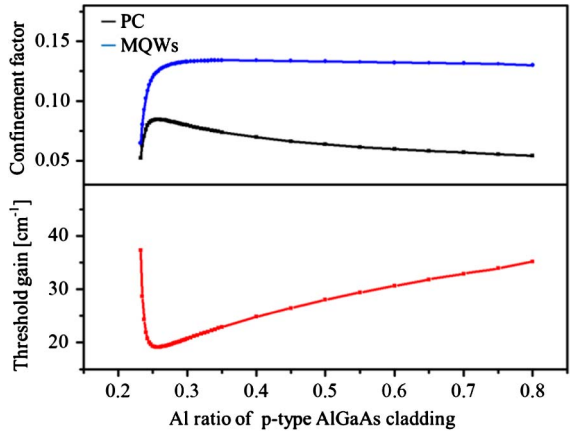

Fig. 4. Threshold gain and confinement factor as a function of the p-cladding Al composition.

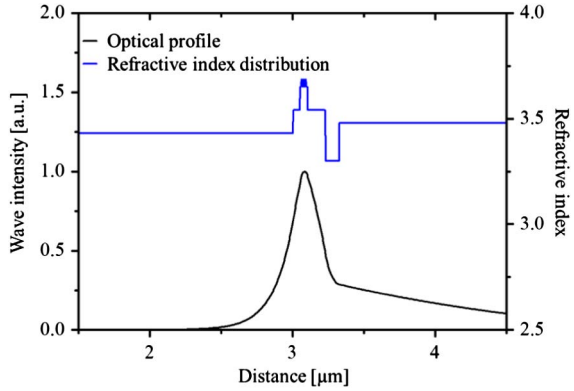

Fig. 5. Optical profile of the device in the vertical direction. The black and blue lines represent the distribution of the optical mode profile and the corresponding refractive index under the design of the PC structure, respectively. The optical profile obviously moves toward the p-cladding layer and enhances the overlap with the PC layer.

reduced less than 0.26. Under this regime, the optical field distribution starts to move away from the QWs quickly, and most of the mode profiles prefer to distribute in the p-type cladding layer. It not only causes a significant raise in the threshold gain of the fundamental mode, but it also increases the probability of nonradiative recombination in the p-type AlGaAs materials due to the severe free-carrier absorption. Hence, we find that the corresponding threshold gains exhibit a tendency that is opposite the confinement factor as a function of the p-cladding Al composition, and they reach a critically minimum value at the composition of $Al_{0.26}Ga_{0.74}As$. The corresponding optical field distribution of the optimized confinement factor is shown in Fig. 5.

Adopting the optimal p-type AlGaAs composition, we also try to modify the filling factor to observe again its influence on the threshold gain. The results are presented in Fig. 6. The minima values of the threshold gains occur at two valleys of the corresponding curve, which are, respectively, located at 0.09 and 0.55. For the square-lattice PC lasers with TE polarization, the coupling constant is decided from the coupling effect of two plane waves propagating at 45° and 180°. However, the intensity of the coupling of the planes propagating in the directions perpendicular to each other does not exist in the model. As we increase the radius of the hole to raise the filling factor from 0 to 0.09, both coupling constants propagating in the 45° and 180° directions are enhanced simultaneously, and hence the threshold gain is reduced to reach a valley point. While the filling factor increase closed to 0.3, the degree of backward diffraction becomes very small, and there is insufficient optical confinement. Therefore, the threshold gain curve exhibits a peak value with 345 cm^{-1} at $f = 0.3$. As we keep increasing the filling factor from 0.3 to 0.55, the coupling effect of the plane waves propagating at 45° continues to grow and become the dominating factor of the coupling constant. We can still obtain the second valley point at $f = 0.55$, although the backward diffraction forms a destructive interference with the coupling propagating in the 45° directions. Under these alterations of the filling factor, the strength of the coupling between the optical field and the PC is also distinct. The filling factor at 0.09 for the lowest threshold gain calculated to be 21.36 cm^{-1} could be referred to as the best parameter of the optical coupling to effectively decrease the threshold gain of the PCSEL.

In order to obtain the ultimately optimized threshold gain, we use the above-mentioned design and gradually adjust the Al composition of the p-type AlGaAs cladding layer and PC filling factor simultaneously to yield the 2D mapping of the threshold gain with a natural logarithm scale under this AlGaAs-based PCSEL structure (as shown in Fig. 7), thus exhibiting the threshold gain as a function of the Al composition and filling factor. We can find that the best result occurs when the values of the filling factor and Al content are 0.07 and 0.27, respectively. The threshold gain is calculated to be around 19.45 cm^{-1}, which is much lower than the threshold gain of 50 cm^{-1} for the conventional PCSEL with a

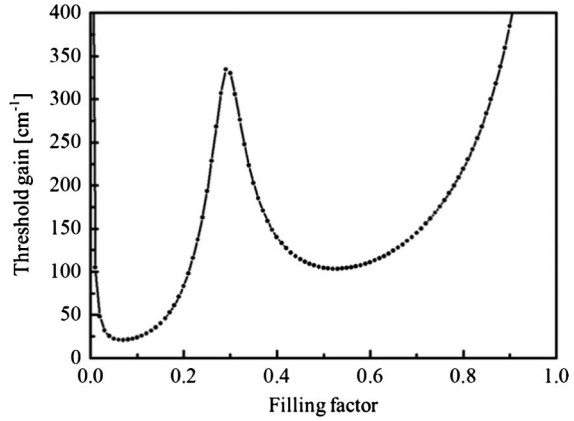

Fig. 6. The relationship between the threshold gain and the filling factor utilized in the optimal p-cladding Al composition shown in Fig. 4.

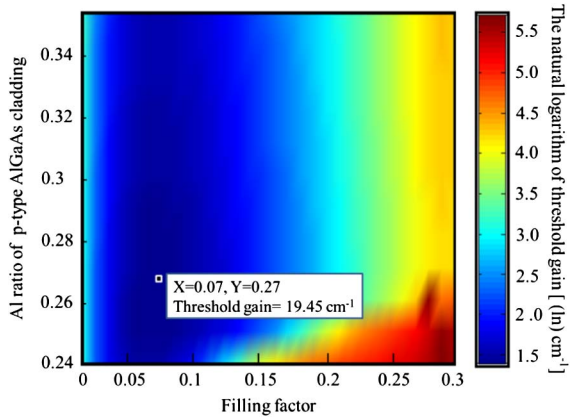

Fig. 7. Threshold gain as a function of the PC filling factor and Al content of the p-type AlGaAs cladding layer whose variation is indicated by the color alteration.

symmetric cladding structure. Moreover, the optical confinement factor of the PC region in the vertical direction can be enhanced to as high as 13.94% through the above optimization procedure. Comparing to the nonoptimized structure design shown in Fig. 2, we believe that the proportion of overlap between the optical mode profile and the PC layer is indeed increased by using the asymmetric cladding design. It obviously contributes to the improvement of the coupling effect on the PC region, and hence, it lowers the threshold gain of the PCSLEs.

4. Conclusion

In conclusion, we have presented the effect of an asymmetric cladding design on the vertical optical confinement by the TMM, and optimized the structure design of a PCSEL to calculate the lowest value of threshold gain by the CWT. Both the influences of the threshold gain and filling factor have been considered simultaneously. Under a suitable structure modification, the optimized filling factor of the PC was calculated as 0.07. It resulted that the optical confinement factor of the PC region in the vertical direction could rise dramatically when the Al content decreased from 0.3 to 0.27. Finally, the best value of the vertically optical confinement factor of the PC in the optimized AlGaAs-InGaAs PCSELs was calculated as 13.94%, and the corresponding threshold gain was reduced to 19.45 cm^{-1}. This study demonstrated that the asymmetric cladding design offered a better device characteristic than those of traditional symmetric structure by adopting this effective optimization procedure in the design of PCSEL structures.

References

1. M. Imada, S. Noda, A. Chutinan, T. Tokuda, M. Murata, and G. Sasaki, "Coherent 2-D lasing action in surface-emitting laser with triangular lattice photonic crystal structure," Appl. Phys. Lett. **75**, 316–318 (1999).
2. S. Noda, M. Yokoyama, M. Imada, A. Chutinan, and M. Mochizuki, "Polarization mode control of 2-D photonic crystal laser by unit cell structure design," Science **293**, 1123–1125 (2001).
3. H. Y. Ryu, S. H. Kwon, Y. J. Lee, and J. S. Kim, "Very-low-threshold photonic band-edge lasers from free-standing triangular photonic crystal slabs," Appl. Phys. Lett. **80**, 3476–3478 (2002).
4. G. A. Turnbull, P. Andrew, W. L. Barns, and I. D. W. Samuel, "Operating characteristics of a semiconducting polymer laser pumped by a microchip laser," Appl. Phys. Lett. **82**, 313–315 (2003).
5. T. C. Lu, S. W. Chen, L. F. Lin, T. T. Kao, C. C. Kao, P. C. Yu, H. C. Kuo, S. C. Wang, and S. H. Fan, "GaN-based 2-D surface-emitting photonic crystal lasers with AlN/GaN distributed Bragg reflector," Appl. Phys. Lett. **92**, 011129 (2008).
6. T. C. Lu, S. W. Chen, T. T. Kao, and T.-W. Liu, "Characteristics of GaN-based photonic crystal surface emitting lasers," Appl. Phys. Lett. **93**, 111111 (2008).
7. S. W. Chen, T. C. Lu, Y. J. Hou, T. C. Liu, H. C. Kuo, and S. C. Wang, "Lasing characteristics at different band edges in GaN photonic crystal surface emitting lasers," Appl. Phys. Lett. **96**, 071108 (2010).
8. E. Miyai, K. Sakai, T. Okano, W. Kunishi, D. Ohnishi, and S. Noda, "Lasers producing tailored beams," Nature **441**, 946 (2006).
9. M. Imada, A. Chutinan, S. Noda, and M. Mochizuki, "Multidirectionally distributed feedback photonic crystal lasers," Phys. Rev. B **65**, 195306 (2002).
10. M. Yokoyama and S. Noda, "Finite-difference time-domain simulation of two-dimensional photonic crystal surface-emitting laser," Opt. Express **13**, 2869–2880 (2005).
11. I. Vurgaftman and J. R. Meyer, "Design optimization for high-brightness surface-emitting photonic-crystal distributed-feedback lasers," IEEE J. Quantum Electron. **39**, 689–700 (2003).
12. H. Kogelnik and C. V. Shank, "Coupled-wave theory of distributed feedback lasers," J. Appl. Phys. **43**, 2327–2335 (1972).
13. K. Sakai, E. Miyai, and S. Noda, "Coupled-wave theory for square lattice photonic crystal lasers with TE polarization," IEEE J. Quantum Electron. **46**, 788–795 (2010).
14. C. T. Hung, Y. C. Syu, T. T. Wu, and T. C. Lu, "Design of low-threshold photonic crystal surface-emitting lasers," IEEE Photon. Technol. Lett. **24**, 866–868 (2012).